Early Alveolar Epithelial Cell Necrosis is a Potential Driver of ARDS with COVID-19

Kentaro Tojo, Natsuhiro Yamamoto, Nao Tamada, Takahiro Mihara, Miyo Abe, Takahisa Goto

Online Data Supplement

Supplementary Figures

Supplementary Figure E1

Pearson correlation coefficients among circulating markers; soluble receptors for advanced glycation end products (sRAGE), angiopoietin (ANG)-2, surfactant protein-D (SP-D), cytokeratin (CK)18-M65, CK18-M30 and high mobility group box (HMGB)-1.

The serum levels of each marker were log-transformed and then Pearson's correlation analyses were performed.

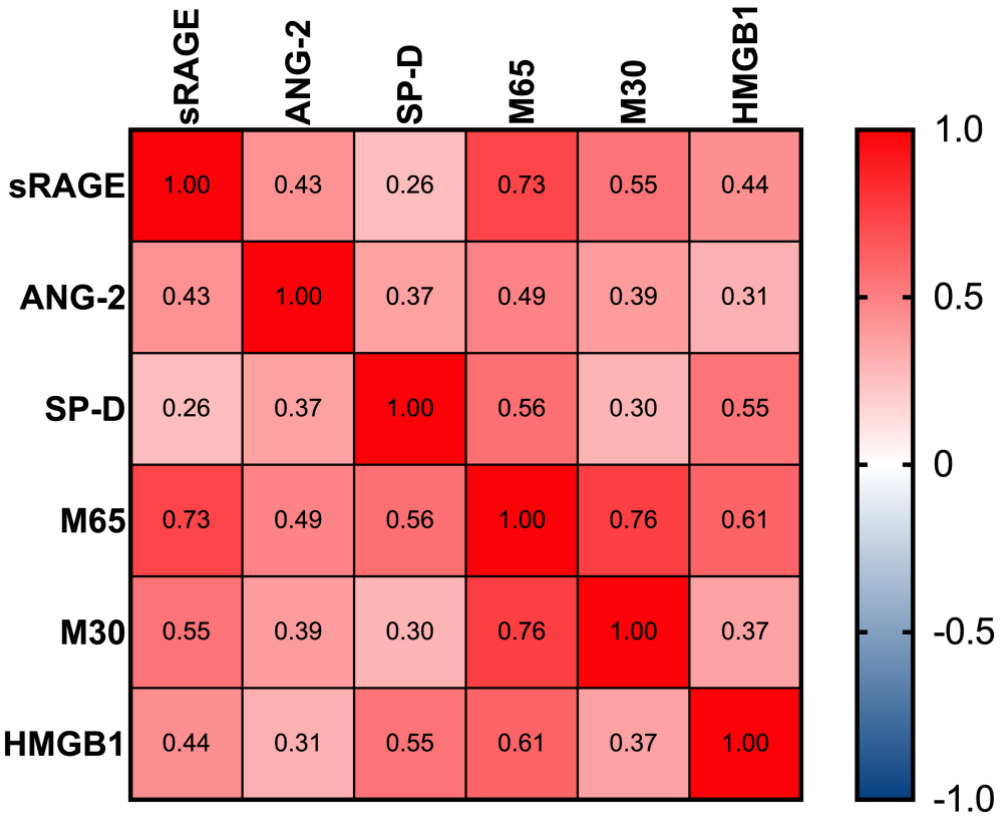

Supplementary Figure E2

Intratracheal administration of the severe acute respiratory syndrome coronavirus 2 (SARS-CoV-2) spike protein combined with polyinosinic:polycytidylic acid (poly (I:C)). Levels of (A) white blood counts and (B) total proteins in the bronchoalveolar lavage fluid of mice intratracheally injected with phosphate buffered saline, poly (I:C) or SARS-CoV-2 spike proteins combined with poly (I:C) are shown. (C) Representative images of lung tissue sections stained with hematoxylin and eosin. The values were presented as means ± standard error. *p<0.05, **p<0.01, ***p<0.0001.

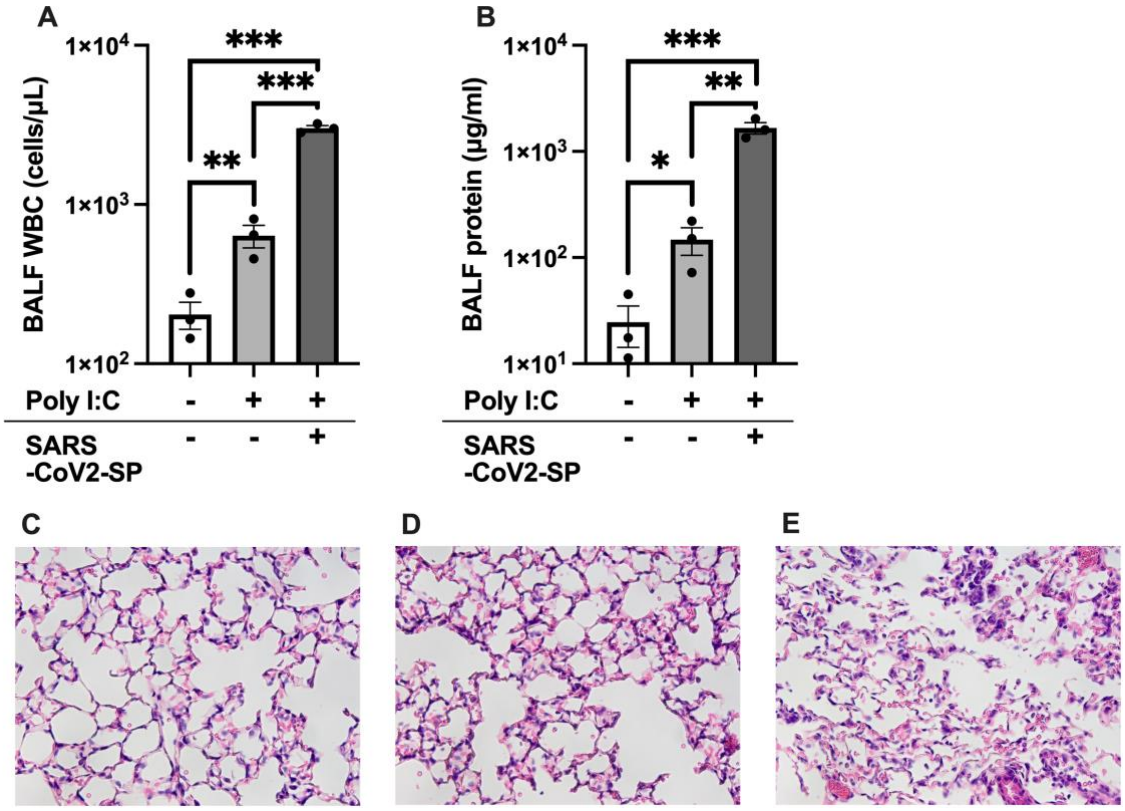

Supplementary Figure E3

Loading controls for immunoblots. Equality of protein loading was confirmed by beta-actin staining (in case of protein amounts <10 μg) or total protein staining (in case of protein amounts >10 μg). Immunoblot images of (A) mixed lineage kinase domain-like (MLKL) and (B) gesdermin D (GSDMD) membranes treated with anti-beta actin antibodies are shown. Total protein-stained membranes of (C) phosphorylated MLKL and (D) cleaved GSDMD are shown.

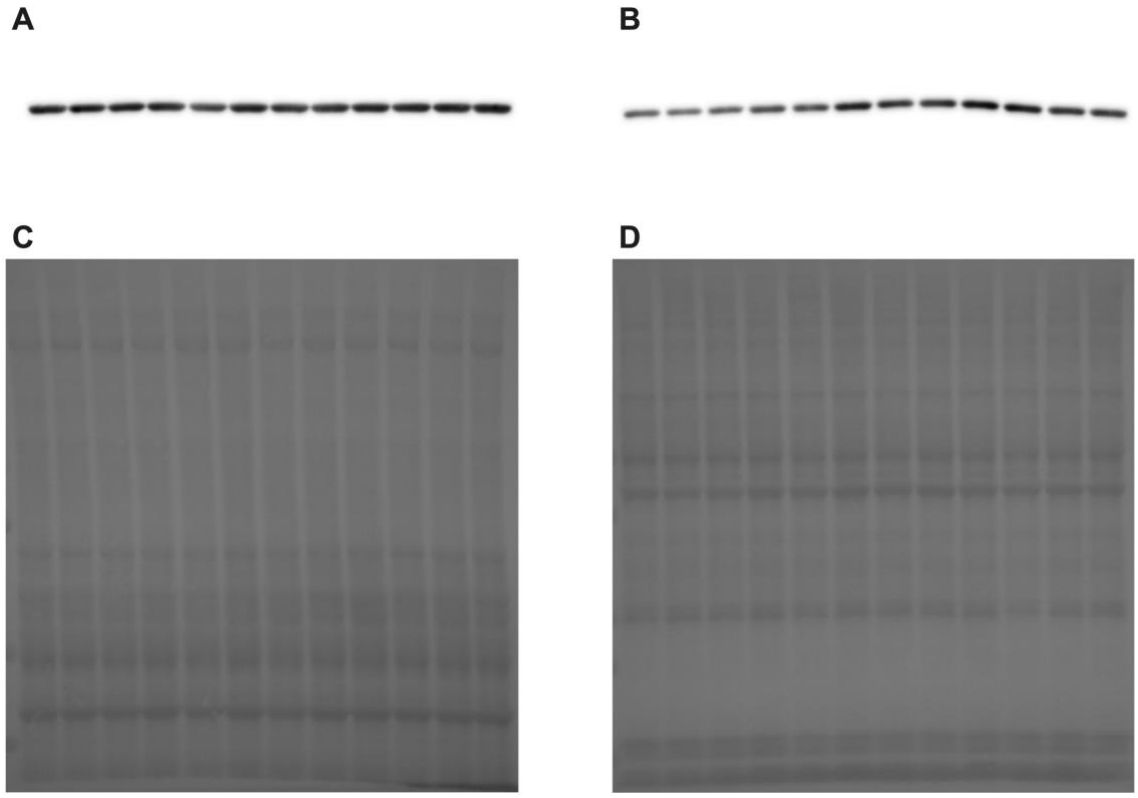

Supplementary Text E1

Supplementary methods

Clinical study design

In this single-center, retrospective, prospective observational study, we analyzed serum samples of adult patients with coronavirus disease (COVID-19) who were admitted to Yokohama City University Hospital from January 2020 to January 2021and healthy controls matched as closely as possible for age and sex. Inclusion criteria for COVID-19 patients were, as follows: 1) a diagnosis of COVID-19 based on a positive real-time polymerase chain reaction test, 2) age ≥ 18 years, and 3) available residual serum samples. Acute respiratory distress syndrome (ARDS) was diagnosed based on the Berlin definition. The study protocol was reviewed and approved by the institutional review board of Yokohama City University Hospital (B200700100). The requirement for informed consent was waived due to the observational nature of the study. Some preliminary data from retrospectively collected samples were previously published(1).

Clinical data collection

The following clinical data measured during the first 8 days of hospital admission were retrospectively collected from the medical charts of included patients: basal characteristics, vital signs, laboratory tests, and blood gas analysis findings.

Human serum sample analysis

Residual serum samples collected from patients with COVID-19 after daily laboratory tests were frozen for future use. Concentrations of human serum soluble receptors for advanced glycation end products (sRAGE) (DY1145, R&D systems, Minneapolis, MN), angiopoietin (ANG)-2 (DY623, R&D Systems), surfactant protein (SP)-D (DY1920, R&D Systems), cytokeratin (CK)18-M65 (M65 ELISA, #10020, VLVBio AB, Nacka, Sweden), CK18-M30 (M30-Apoptosense ELISA Kit, #10011, VLVBio), and high mobility group box (HMGB)-1 (#381-10531, Fuso, Osaka, Japan) were measured using commercially available enzyme-linked immunosorbent assay (ELISA) kits according to the manufacturer's instructions. The ratio of CK18-M30/M65 was calculated, and when the value exceeded 100%, it was regarded as 100%.

Initial concentrations of these markers in ARDS and non-ARDS patients at admission (on the first or second hospital day) and healthy controls were compared. Further, temporal changes in levels of the markers were assessed in patients with ARDS

throughout the 8-day period following hospital admission. In cases in which values were determined twice per day, mean values were used. In cases in which only a single value was available, the value was used.

Animal experiments

All animal experimental protocols were approved by the Animal Research Committee of the Yokohama City University. Male specific-pathogen-free C57BL/6J mice aged 8–10 weeks that were purchased from Japan SLC (Shizuoka, Japan) were used for all animal experiments. Mice were housed under a 12-h light/dark cycle with food and water available ad libitum. Intratracheal administration of polyinosinic:polycytidylic acid (poly (I:C)) (P1530, Sigma-Aldrich, St. Louis, MO, USA) with or without the severe acute respiratory syndrome coronavirus 2 (SARS-CoV-2) spike protein (Z03481, Lot B2103045, GenScript, Piscataway, NJ) was performed via the exposed trachea through a small incision at the front of the neck. During the procedure, mice were placed under general anesthesia using intraperitoneal ketamine and xylazine. Mice were euthanized 24 h after intratracheal instillation, and lung tissues and bronchoalveolar lavage fluid (BALF) samples were collected as previously described(2, 3).

In a preliminary experiment, nine mice were randomly allocated into the following three groups (n = 3 per group): control, Poly (I:C), and Poly (I:C) combined with the SARS-CoV-2 spike protein. The poly (I:C) group received 250 μg intratracheal poly (I:C) dissolved in 100 μL phosphate buffered saline (PBS), and poly (I:C) combined with SARS-CoV-2 group received 50 μg SARS-CoV-2 spike protein with 250 μg poly (I:C) dissolved in 100 μL PBS. The control group received 100 μL PBS intratracheally.

Based on the results of preliminary experiments, mild and severe lung injuries mimicking COVID-19 were evaluated. Twelve animals were randomly allocated into the following three groups (n = 4 per group): control, mild COVID-19, and severe COVID-19. The severe COVID-19 group received 50 μg SARS-CoV-2 spike protein with 250 μg poly (I:C) dissolved in 100 μL PBS, whereas the mild COVID-19 group received 10 μg SARS-CoV-2 spike protein and 50 μg Poly (I:C) in 100 μL of PBS. The control group received 100 μL PBS intratracheally.

Finally, we evaluated effects of anti-HMGB-1 neutralizing antibodies on a severe COVID-19 animal model. Six animals were randomly allocated to anti-HMGB-1 antibody or isotype control groups (n = 3 per group). The severe COVID-19 animal model was established as described above. Then, 4 h after intratracheal instillation, 100 μg anti-HMGB-1 neutralizing (ARG66714, Arigo Biolaboratories, Hsinchu City,

Taiwan) or isotype control antibodies dissolved in 100 μL PBS were intravenously administered via the tail vein under isoflurane anesthesia.

Analysis of the BALF of mouse models of COVID-19

Leukocytes from the BALF of mice were stained with Samson's solution and counted. Protein concentrations in BALF were quantified using a bicinchoninic acid assay. Concentrations of sRAGE (DY1179, R&D systems), ANG-2 (MANG20, R&D systems), CK18-M30 (CSB-E14265M, CUSABIO, Houston, TX), CK18-M65 (CSB-E17158M, CUSABIO), and HMGB-1 (ARG81310, Arigo Biolaboratories) were measured using ELISA kits in accordance with the manufacturer's instructions. Cytokines and chemokines were comprehensively analyzed using semiquantitative multiplex cytokine assay kits (ARY006, R&D systems) in accordance with the manufacturer's instructions.

Western blotting

Total proteins from mouse lung tissues were extracted using trichloroacetic acid-acetone. Extracted proteins were solubilized. Thereafter, they were quantified using a bicinchoninic acid assay. Proteins were detected using primary antibodies against mixed

lineage kinase domain-like (MLKL) (#28640, Cell Signaling Technology, Danvers, MA, dilution: 1:2000), pospho-MLKL (#37333, Cell Signaling Technology, 1:1000), gasdermin D (GSDMD) (ab219800, Abcam, Cambridge, UK, 1:3000), cleaved n-terminal GSDMD (A20197, ABclonal, Woburn, MA, 1:1000) and horseradish peroxidase-conjugated secondary goat anti-rabbit IgG antibodies (170-6515; Bio-Rad, Hercules, CA) as described previously(2). Briefly, a certain amount of protein (MLKL: 5 μg, GSDMD: 2 μg, pMLKL: 30 μg, and cleaved GSDMD: 20 μg of proteins) was separated by sodium dodecyl sulphate-polyacrylamide gel electrophoresis, and transferred to polyvinylidene fluoride (PVDF) membranes. Equality of protein loading was confirmed by total protein staining (in case of protein amounts >10 μg) (Reversible Protein Stain Kit for PVDF Membranes, 24585, Thermo Fisher Scientific, Waltham, MA) or beta-actin (A5411, Sigma-Aldrich, 1:10000) staining (in case of protein amounts <10 μg). The density of each protein was determined using ImageJ software (National Institutes of Health, Bethesda, MD).

Histological analysis

Lung tissues of mice were fixed using 4% paraformaldehyde at 20 cm H_2O pressure and embedded in paraffin for histopathological examination, as previously

described(2). Lung tissue sections were stained with hematoxylin and eosin for tissue injury evaluation. Lung tissue sections were stained with anti-pMLKL (ET1705-51, HUABIO, Woburn, MA, dilution: 1:100) and anti-GSDMD n-terminal (ER1901-37, HUABIO, 1:200) antibodies according to the manufacturer's instructions.

Statistical analysis

Statistical analyses were performed using Prism 9 software (GraphPad, La Jolla, CA). Values of $P < 0.05$ were considered statistically significant. Data from clinical studies were presented as medians with interquartile ranges (IQRs), and analyzed as non-parametric data. Comparisons between basal characteristics and laboratory and physiological values among patients with and without ARDS were performed using Mann-Whitney or Fisher's exact tests. Comparisons of the serum levels of tissue injury and cell death markers among patients with and without ARDS, and healthy controls were performed using Kruskal-Wallis analysis followed by Dunn's multiple comparison test. Temporal changes in alveolar tissue injury markers were assessed using the Friedman test, and days in which alveolar tissue injury markers peaked were compared using Kruskal-Wallis analysis followed by Dunn's multiple comparison test.

Data obtained from animal experiments were log-transformed and presented as means ± standard deviation. Data were analyzed using the Student's t-test or one-way analysis of variance followed by Tukey's multiple comparison test. Multiple cytokine and chemokine assays were analyzed using multiple t-tests via the false discovery rate approach comprised of the two-stage step-up method of Benjamini, Krieger, and Yekutieli(4). The false discovery rate was set at 5%.

References

1. Tojo K, Yamamoto N, Mihara T, Abe M, Goto T. Distinct temporal characteristics of circulating alveolar epithelial and endothelial injury markers in ARDS with COVID-19. *Crit Care* 2021;25:169.

2. Tojo K, Tamada N, Nagamine Y, Yazawa T, Ota S, Goto T. Enhancement of glycolysis by inhibition of oxygen-sensing prolyl hydroxylases protects alveolar epithelial cells from acute lung injury. *Faseb J* 2018;32:2258–2268.

3. Tamada N, Tojo K, Yazawa T, Goto T. Necrosis Rather Than Apoptosis is the Dominant form of Alveolar Epithelial Cell Death in Lipopolysaccharide-Induced Experimental Acute Respiratory Distress Syndrome Model. *Shock* 2020;54:128–139.

4. Benjamini Y, Krieger AM, Biometrika DY. Adaptive linear step-up procedures that control the false discovery rate. *Biometrika* 2006;93:491–507.